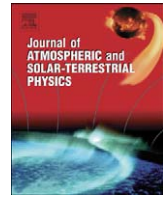




Contents lists available at ScienceDirect

Journal of Atmospheric and Solar-Terrestrial Physics

journal homepage: www.elsevier.com/locate/jastp

Regional millennial trend in the cosmic ray induced ionization of the troposphere

I.G. Usoskin^{a,*}, I.A. Mironova^b, M. Korte^c, G.A. Kovaltsov^d

^a Sodankylä Geophysical Observatory (Oulu unit), 90014 University of Oulu, Finland

^b Institute of Physics, St. Petersburg State University, Russia

^c Helmholtz Centre Potsdam, GFZ German Research Centre for Geosciences, Potsdam, Germany

^d Ioffe Physical-Technical Institute, St. Petersburg, Russia

ARTICLE INFO

Article history:

Received 1 September 2009

Accepted 18 October 2009

Keywords:

Paleomagnetism

Cosmic rays

Atmosphere

Climate

Holocene

ABSTRACT

Long-term trends in the tropospheric cosmic ray induced ionization on the multi-millennial time scale are studied using the newly released paleomagnetic reconstruction models. Spatial and temporal variations of the tropospheric ionization has been computed using the CRAC:CRII model and applying the paleomagnetic CALS7k.2 reconstruction. It has been shown that long-term variations of the tropospheric ionization are not spatially homogeneous, and they are defined not only by solar (i.e., covariant with solar irradiance) changes but also by the geomagnetic field. The dominance of the two effects is geographically separated, which makes it possible to distinguish between direct and indirect solar-terrestrial climate effects. Possible climate applications are considered.

© 2009 Elsevier Ltd. All rights reserved.

1. Introduction

During the pre-industrial epoch, influence of outer space factors on the terrestrial climate may be significant. Most apparent external climate drivers are related to the orbital forcing, resulting in the changing insolation, which can be straightforwardly included into paleoclimatic studies (e.g., Haigh et al., 2005). Possible relations between solar variability and climate on multi-millennial time scale are intensively discussed but their causes are not resolved (e.g., Bond et al., 2001; Xiao et al., 2002; Hong et al., 2001; Niggemann et al., 2003; Haigh et al., 2005; Bard and Frank, 2006). In particular, large uncertainties remain in reconstructions of the long-term solar irradiance (total or spectral) and its effect upon climate (e.g., Haigh et al., 2005; Foukal et al., 2006). Another important factor of the outer space influence upon the terrestrial environment is formed by cosmic rays (e.g., Dorman, 2004; Usoskin and Kovaltsov, 2008). Cosmic rays (CR) are often considered as simply inverted solar activity, due to the heliospheric modulation. However, this is true only on a relatively short time scale, shorter than a century. On longer scales, centennial to millennial, CR flux at the Earth is greatly affected also by changes of the geomagnetic field (e.g., Christl et al., 2004; Usoskin et al., 2008) or, at geological time scales, even by the changing galactic surrounding (Scherer et al., 2006). Accordingly, variations of CR in the Earth's atmosphere can be

essentially different from solar activity on longer time scales, leading to potentially distinguishable effects on the terrestrial environment. In this context, variations of the geomagnetic field and the ensuing CR variations are sometimes considered as an independent possible external driver for the climate (cf. Gallet et al., 2005, 2006; Hyodo et al., 2006; Courtillot et al., 2007; Kitaba et al., 2009; Knudsen and Riisager, 2009). In this paper we emphasize that separating different outer factors may shed new light on our understanding of the natural external drivers of the pre-industrial climate.

The most important terrestrial effect of CR is related to the ionization of the ambient air (Bazilevskaya et al., 2008), which is called the cosmic ray induced ionization (CRII). Cosmic rays form the main source of ionization in the low-to-middle atmosphere, and therefore their variability directly affects such atmospheric conditions as ion concentration and conductivity. On the other hand, these direct atmospheric effects may result in further atmospheric changes, which are potentially capable of affecting climate. Such potential mechanisms include enhanced aerosol and cloud formation in the troposphere, mediated by CR (see, e.g., Marsh and Svensmark, 2003; Scherer et al., 2006; Kazil et al., 2006, 2008; Arnold, 2008; Mironova et al., 2008; Tinsley, 2008). Although details of these mechanisms remain unclear, giving rise to some scepticism (e.g., Bard and Frank, 2006), it could be expected that enhanced CRII would correspond to a larger amount of tropospheric clouds, and thus to colder and wetter regional climate. This link may be partly responsible for the long-term solar-climate influence (e.g., Van Geel et al., 1999; de Jager, 2005; Versteegh, 2005), in concurrence with other solar factors, such

* Corresponding author. Fax: +358 8 553 1390.

E-mail address: ilya.usoskin@oulu.fi (I.G. Usoskin).

as total or spectral solar irradiance (e.g., Haigh and Blackburn, 2006).

It has been discussed (Marsh and Svensmark, 2003; Pallé et al., 2004; Usoskin et al., 2006; Voiculescu et al., 2006) that the relation, if existing, between different types of cloud and CRII has clear regional dependence and can be hardly presented as an overall global link, especially on the annual to decadal time scales. On the other hand, long-term (centennial) changes in CRII can also be different in different regions, affected by the fast geomagnetic axis migration (Kovaltsov and Usoskin, 2007; Usoskin et al., 2008). In this paper we study regional changes of the tropospheric CRII over the last 6–7 millennia and show the importance of the geomagnetic field variations. We also provide, as a possible implication of the millennial CRII regional variations, a statistical comparison between regional paleoclimatic (lake status) reconstructions and the computed tropospheric CRII variations. Such a study may shed a new light on the role, if any, of cosmic rays on the long-term regional climate variations.

Here we concentrate on the long-term studies for the pre-industrial epoch without essential anthropogenic factors. We note that any advance in the knowledge of natural external climate forcing may lead to a progress in our understanding of the man-made effects during the modern epoch.

2. Cosmic ray induced ionization

Cosmic rays, mostly of galactic origin, are highly energetic particles, permanently impinging upon the Earth's atmosphere. They initiate a complicated nucleonic–electromagnetic cascade in the atmosphere, which can affect its physical–chemical conditions. Cosmic ray induced ionization is a result of the cascade induced by energetic cosmic rays in the Earth's atmosphere. The ionization rate at a given location and altitude h can be expressed as (Usoskin et al., 2004):

$$Q = \sum_i \int_{T_{c,i}}^{\infty} J_i(T, \phi) Y_i(h, T) dT, \quad (1)$$

where summation is over different species of primary CR, J_i is the differential energy spectrum of the i th specie of CR near Earth outside the geomagnetic field, and $Y_i(h, T)$ is the ionization yield function. Integration is over the kinetic energy T above $T_{c,i}$, which is the kinetic energy corresponding to the local vertical geomagnetic cutoff rigidity P_c . Assuming the constancy of the chemical composition and physical properties of the atmosphere, one can see that the CRII temporal variations (at a given altitude) are controlled by two mutually independent factors: local geomagnetic cutoff, defined by the geomagnetic field; and differential energy spectrum of CR outside the magnetosphere. In this study we use CRII as computed by a CRAC (Cosmic Ray induced Atmospheric Cascade) full 3D numerical model (Usoskin and Kovaltsov, 2006), whose validity for the troposphere and stratosphere has been verified in different conditions (Usoskin et al., 2009). The CRAC:CRII model computes CRII at a given altitude as function of the CR energy spectrum, parameterized via the heliospheric modulation potential ϕ , and the local geomagnetic rigidity cutoff P_c .

Since the interstellar CR spectrum can be regarded as constant on the millennial time scale (Scherer et al., 2006), all changes in the CR spectrum near Earth are ascribed to the modulation of CR in the heliosphere, ultimately determined by the solar magnetic activity (Usoskin and Kovaltsov, 2004). For long-term studies it is common to parameterize the CR energy spectrum using the only time variable parameter, the modulation potential ϕ , in the framework of the force field approximation (see the full formalism in Usoskin et al., 2005b). Here we use a recent

reconstruction of the modulation potential over the last 7000 years from the data on cosmogenic ^{14}C (Usoskin et al., 2007). This reconstruction is based on the same paleomagnetic model CALS7K.2 as we use here, thus minimizing possible systematic errors due to uncertainties of the geomagnetic field reconstruction. The temporal variability of the reconstructed modulation potential since 4000 BC is shown in Fig. 1A. The long-term trend in the solar modulation of CR was negative, the modulation being gradually decreasing between 2000 BC and the Spörer minimum of solar activity ca. 1500 AD. The modulation was quickly increasing since the Maunder minimum ca. 1700 AD until present, but this plays only a little role in the multi-millennial trend.

Shielding effect of the geomagnetic field hampers CR particles from reaching the atmosphere (e.g., Smart et al., 2000; Kudela and Usoskin, 2004). In a simple form, well suitable for long-term studies, the geomagnetic shielding can be parameterized via the

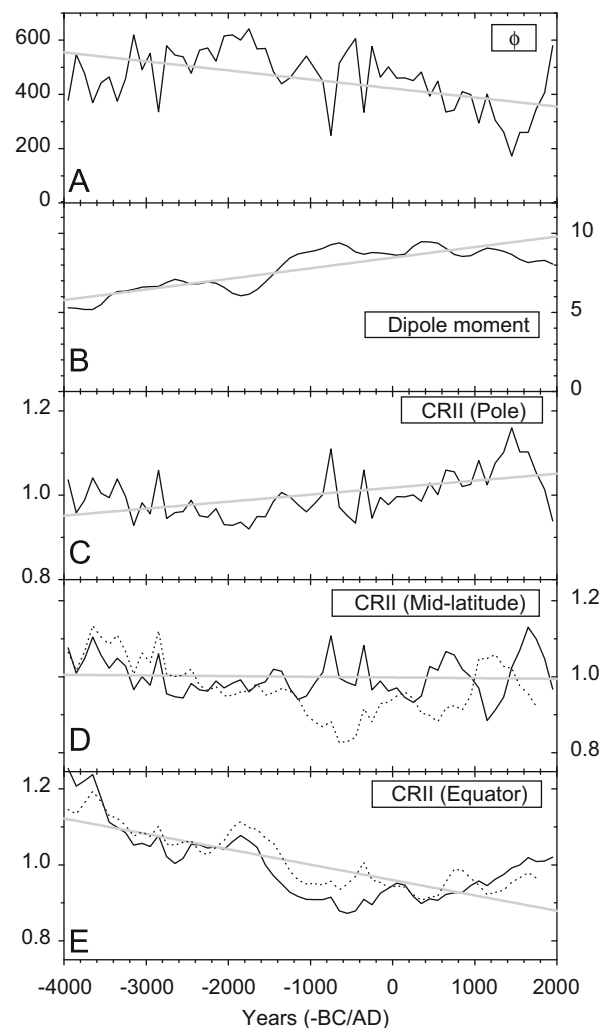


Fig. 1. Time profiles for the last 6000 years (all data are averaged over calendar centuries). Panel A: Cosmic ray modulation potential ϕ (in MV), reconstructed from the cosmogenic ^{14}C data by Usoskin et al. (2007). Panel B: Geomagnetic dipole moment M (in 10^{22} A m^2), computed from the CALS7K.2 model (Korte and Constable, 2005, 2008). Panel C: Normalized cosmic ray induced ionization in the middle troposphere (residual atmospheric depth 500 g/cm^2 or the altitude of about 5.8 km), computed using the CRAC:CRII model (see text for details; Usoskin and Kovaltsov, 2006) for the polar region ($72^\circ \text{ N } 0^\circ \text{ E}$). Panel D: The same as panel C but for mid-latitudes ($45^\circ \text{ N } 0^\circ \text{ E}$ —solid line, $45^\circ \text{ N } 180^\circ \text{ E}$ —dotted line). Panel E: The same as panel C but for the equator ($0^\circ \text{ N } 0^\circ \text{ E}$ —solid line, $0^\circ \text{ N } 180^\circ \text{ E}$ —dotted line). Gray lines depict the best-fit linear trend, computed for the solid curve, in each panel.

geomagnetic cutoff rigidity P_c , which implies a low bound of rigidity a CR particle must possess in order to reach the atmosphere (Cooke et al., 1991). Most important for the geomagnetic shielding is the dipole component of the magnetic field, since higher moments decay more rapidly with distance from the source. In the dipole approximation, the geomagnetic vertical cutoff rigidity is evaluated using the Störmer's equation (Elsasser et al., 1956):

$$P_c \approx 1.9 \cdot M \left(\frac{Ro}{R} \right)^2 \cos^4 \lambda_G, \quad (2)$$

where M is the geomagnetic dipole moment (in 10^{22} Am^2), Ro is the Earth's mean radius, and R and λ_G are the distance from the given location to the dipole center and the angular distance to the magnetic pole (geomagnetic latitude), respectively, and P_c is expressed in GV. Here we use a model of the eccentric dipole, which takes into account the quadrupole contributions from a standard spherical harmonic description and is a good approximation to the reality at the relevant distance from the Earth (Webber, 1962; Fraser-Smith, 1987). The eccentric dipole has the same dipole moment and orientation of the axis as the centered dipole, but the center of the dipole and consequently the poles defined as the points where the axis crosses the surface are

shifted with respect to the geographical ones. The first eight Gauss coefficients of a geomagnetic field model are necessary to compute the dipole moment M , geographical coordinates of the dipole center, and the magnetic poles of the eccentric dipole. Details of the P_c computation based on the eccentric dipole model are given in the Appendix.

In order to account for the geomagnetic changes in the past, we make use of a paleomagnetic reconstruction over the last seven millennia provided by the CALS7K.2 model (Korte and Constable, 2005). The variations of the computed dipole moment M are shown in Fig. 1B for the last 6000 years. One can see that the general trend in the dipole moment was increasing: it was nearly doubled during the first half of the studied period, until about 1000 BC, and remained at a high level of $(8-10) \times 10^{22} \text{ Am}^2$ after that. During that time, the magnetic axis was wandering quite essentially at the centennial scale (Korte and Constable, 2008; Usoskin et al., 2008) within the polar cap (geographical latitude above 80°).

Thus, CRII at a given location and time can be affected by variations of both the solar modulation of CR and the geomagnetic field, and their relative role varies over the Globe. Fig. 2 shows scatter plots of the CRII (shown in Fig. 1) versus the two driving parameters, ϕ and M . One can see that, since there is no

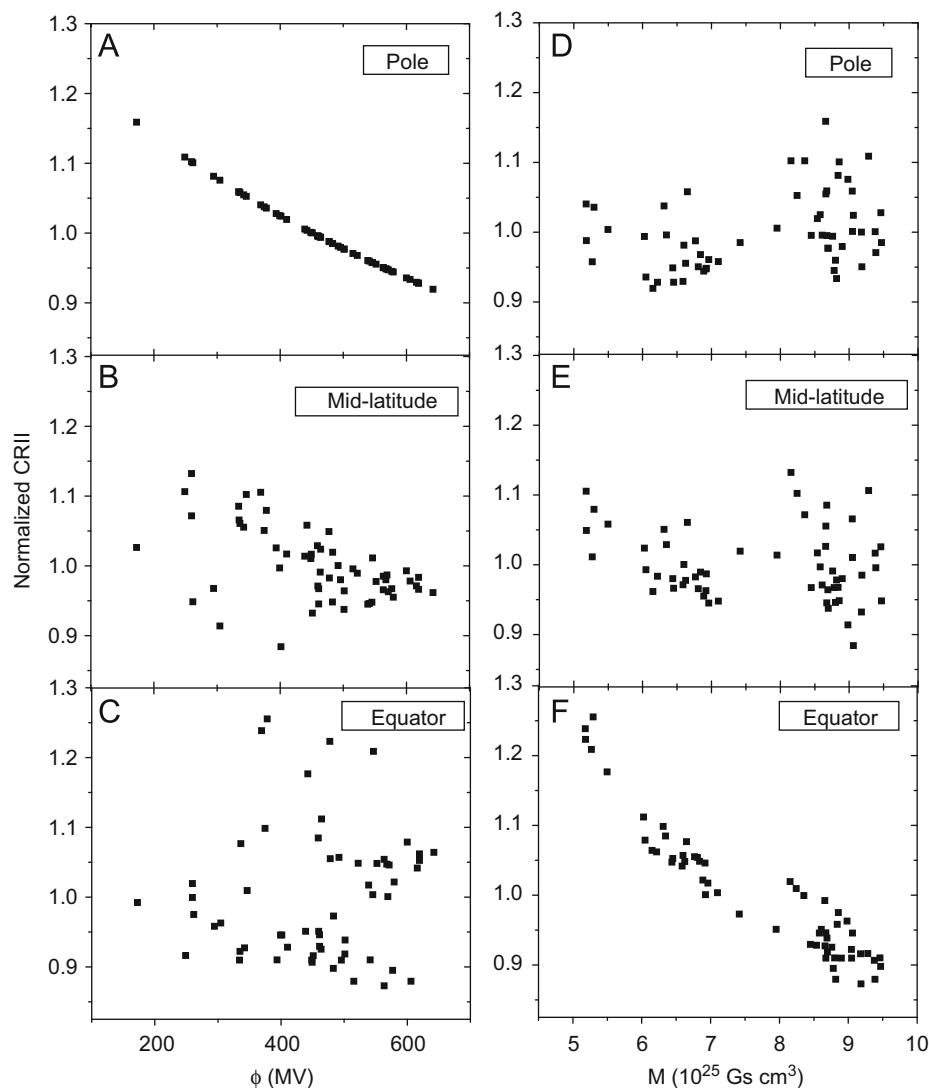


Fig. 2. Dependence of the normalized tropospheric cosmic ray induced ionization on the modulation parameter ϕ (panels A–C) and the geomagnetic dipole moment M (panels D–F) for the last 6000 years. Top, middle and bottom row panels correspond to the polar, mid-latitude and equatorial regions, respectively.

geomagnetic shielding in the polar region, polar CRII is totally defined by the solar modulation (panel A) and is independent of the geomagnetic field (panel D). This relation is reversed in an equatorial region, where the CR variability is mostly defined by the magnetic dipole moment (panel F). The situation at mid-latitudes is more complicated. Both the geomagnetic dipole and solar changes play a role but none of them dominates (panels B and E). Moreover, migration of the geomagnetic axis becomes crucial at mid-latitudes (Kovaltsov and Usoskin, 2007; Usoskin et al., 2008). In order to illustrate the latter, we show in Fig. 1 also the CRII profiles at opposite longitudes (Greenwich and 180° meridians) at different latitudes. There is no longitudinal difference in the polar regions (panel C), and the maximum range of CRII variability between the Medieval maximum and the Maunder minimum is about 20%. Slowly varying difference at the equator (panel E) is caused by a changing offset in the dipole center with respect to the Earth's center with the range of variability being a factor of roughly 1.5. Variations of the CRII at mid-latitudes (panel D) are defined by all the factors: Before ca. 1500 BC, when the magnetic axis was not far from the geographical one, CRII was affected by both ϕ and M , but after that it was mostly dominated by the effect of the geomagnetic axis migration. This can be observed as the anti-phase variations of the CRII at opposite locations (solid and dotted curves) since 1400 BC. Thus, the millennial scale CRII variability can be roughly separated in three regions: Polar region, where the CRII is totally defined by the solar activity changes; Tropical region, where CRII is mostly dominated by changes in the geomagnetic field; Mid-latitude region, where both effects are equally important.

Fig. 3 shows a geographical pattern of the millennial trends in CRII (defined as the slope of the best fit linear trend of the tropospheric CRII variations in each location for the past 6800 years—see panels C–E in Fig. 1). Since the solar activity (Fig. 1A) and geomagnetic field strength (Fig. 1B) depict opposite millennial trends, the above three regions are clearly separated. CRII in polar regions (above $60\text{--}70^\circ$ geographical latitude) shows a weak positive millennial trend (about 0.2% per century), corresponding to the overall decrease of the solar activity. On the other hand, strong negative CRII trend (up to -0.5% per century) is obtained around the (geomagnetic) equator, responding to the increasing geomagnetic moment. At the middle latitudes, the CRII remained at roughly the same level during the last millennia. The globally averaged tropospheric CRII depicts a decreasing trend ($-0.2 \pm 0.03\%$ /century) over the past six millennia. We note that the pattern shown in Fig. 3 would have been different if another time period was chosen.

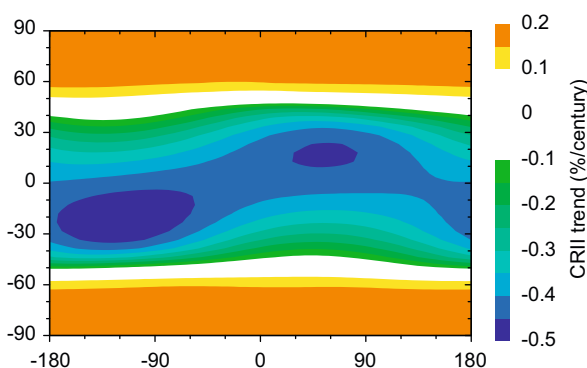


Fig. 3. Spatial pattern ($5^\circ \times 5^\circ$ grids) of the millennial trend in tropospheric cosmic ray induced ionization for the last 6800 years (see text for definition). Color scale to the right represents the slope of the trend in %/century. (For interpretation of the references to color in this figure legend, the reader is referred to the web version of this article.)

Therefore, the global effect of CR upon Earth is defined, at this time scale of several millennia, largely by changes in the geomagnetic field rather than by solar variability.

3. Possible climate implication

In this section we compare long-term trends in CRII with some paleoclimatic proxy as a simple statistical test of a possible relation between CR variability and local climate on long time scales. Since the local/regional variations are essential, we concentrate not on global indices but on some regional paleoclimatic series, such as regional humidity/precipitation indices. While global indices do not allow to clearly distinguish between direct and indirect solar-terrestrial links (e.g., de Jager, 2005; Usoskin et al., 2005a), the use of regional data may help in disentangling the effects, since CRII has a geographical dependence different from that of direct solar influence (insolation). Moreover, regional data are usually more or less homogeneous, while global indices, obtained as spatial average/decomposition of the regional data, may contain inhomogeneities and biases, especially when using spatially sparse original data. In this study we emphasize long-term trends in the data rather than detailed time variability of cosmic rays and terrestrial parameters. Here we only aim to illustrate possible climate implications of the long-term CRII variability by studying only statistical significance of the relations without trying to support or refute any particular mechanism. Neither do we pretend to provide a comprehensive analysis of all the existing climatic data sets, but we want to test the hypothesis of a link by one example first.

We make use of an extensive database, related to the level of precipitation—the global status of lakes around the world during the last 6–7 millennia. This data set, available via the PMIP-2 Project GLSDB (<http://pmip2.lscce.ipsl.fr/pmip2/synth/lakestatus.shtml>), contains the relative status of more than 600 lakes around the world (Kohfeld and Harrison, 2000; Yu et al., 2001; Harrison et al., 2003). Here we analyzed the present status of the lakes compared to that 6800 calendar years ago (originally given as 6000 radiocarbon years). Since the status of a lake is defined by the balance between precipitation and evaporation, the wetter lake status generally correspond to wetter/colder climate, and according to the adopted hypothesis on CR—climate relation, to higher CRII (cf., e.g., Knudsen and Riisager, 2009). For each lake, the relative status is quantified as $L = -2, -1, 0, 1, 2$, according to whether the lake is presently much drier, drier, similar, wetter, and much wetter, respectively, compared to that 6800 years ago. Here we consider only general multi-millennial trends, ignoring detailed temporal comparison of climatic and CR-related data, which has been studied, e.g., by Usoskin and Kovaltsov (2008) for global and by Knudsen and Riisager (2009) for a few regional climate indices.

Since the status of individual lakes may be not mutually independent (closely located sites are expected to depict similar patterns), we averaged the data available in relatively large geographical grid boxed (15° in longitude $\times 10^\circ$ in latitude). Thus defined geographical pattern is shown in Fig. 4 with colors ranging from blue (much drier) to red (much wetter). Lake data exists for 84 out of 432 grid boxes, and the general pattern shows drying in Africa and Asia, wetting in Northern America, and unsettled situation in South America, Europe and Australia. This matrix of the relative lake status can be quantitatively compared, in a statistical manner, to the CRII pattern. The latter is represented by a map of the spatial distribution of the CRII trend slope S (similar to that shown in Fig. 3) but computed for the same geographical grid ($15^\circ \times 10^\circ$) as the lake status (Fig. 4). In each grid box, we computed a product $P = S \times L$ of the lake

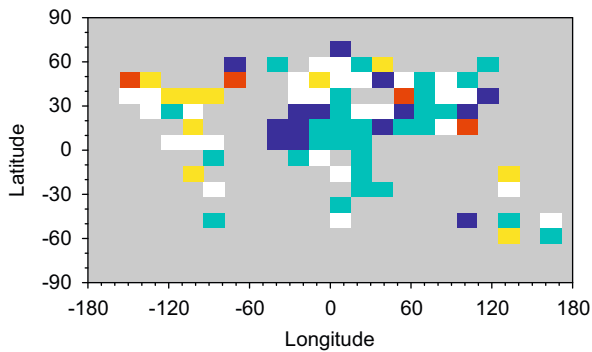


Fig. 4. Spatial pattern of the millennial trend in the lake status (see text for definition). Red, yellow, white, light blue and blue colors correspond to much wetter, wetter, no change, drier and much drier present status, respectively, of the lakes compared to that 6800 BP. Regions without data of the lake status are filled in gray. (For interpretation of the references to color in this figure legend, the reader is referred to the web version of this article.)

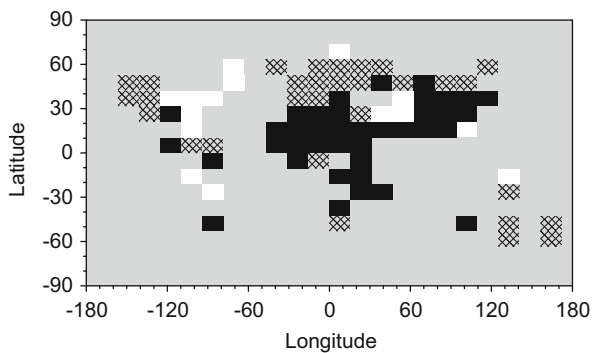


Fig. 5. The agreement P (see text for definition) between millennial trends in the tropospheric cosmic ray induced ionization and in the lake status. Black and white rectangles correspond to regions of agreement and disagreement, respectively. Hatched rectangles depict regions with unsettled relation ($P < 0.1$). Regions without data of the lake status are filled in gray.

status L (if available) and the CRII trend slope S . According to the adopted CR—climate relation, we expect an agreement between the two values (increasing CRII leads to wetter lake status and vice versa). Therefore, we consider the parameter P as a measure of the agreement between the two indices. A map of the distribution of the agreement is shown in Fig. 5 (only the sign of the P is shown). General agreement is observed over the entire Africa and a major fraction of Asia, with a few spots in both Americas and in Australia. Disagreement is observed in a region in Northern America and a few spots in South America, Near East and Oceania. Europe, Alaska and Australia, i.e., the middle-to-high latitude regions, remain uncertain. Visual inspection of the agreement does not allow to evaluate its statistical significance—could it reflect a random pattern or a causal link?

Accordingly, we have performed a statistical test of the result. The average value of $\langle P \rangle$ over all the 84 grid boxes is 0.18 ± 0.04 , i.e., significantly positive, formally implying an agreement between the two sets of trends. However, this value alone can be misleading since the lake status data exists mostly in the low-to-mid latitudes, where the CRII trend is dominantly negative. Therefore, we estimate the significance of this result by a random Monte Carlo method as follows. We took the actual values of the lake status data L but randomly shuffled them inside the existing grid boxes. Then new values of P^* were calculated for these grid boxes, using the actual CRII trends S there, and the average value $\langle P^* \rangle$ was obtained. By repeating this procedure $N = 10\,000$ times, we obtained a distribution of $\langle P^* \rangle$. Finally, the number of

simulations n with $|\langle P^* \rangle| > \langle P \rangle$ gives an estimate of the significance α of the agreement between lake status and CRII trends (the probability that this agreement is due to a random coincidence without a causal link): $\alpha \equiv n/N$. This test yields the significance of $\alpha \approx 0.02$, indicating that the probability of a random occurrence of the observed agreement between lake status and CRII trends is about 2%.

We note that the above test neglects a possible effect of the spatial (regional) correlation between the neighboring grid boxes (closely located lakes are expected to behave similarly). However, due to a large size of the grid boxes, this regional correlation is rather small (about 0.3) for the adjoining grid boxes and diminishes for larger scales.

4. Discussion and conclusions

We have demonstrated that the long-term changes of the cosmic ray induced ionization in the low atmosphere are affected by two major factors: Solar variability, and geomagnetic field changes. While the former factor defines the CRII in the polar region, the latter dominates CRII variability in equatorial regions. CRII variability at middle latitudes is a result of an interplay between the two factors, which are both equally important. Fig. 3 presents a geographical pattern of the long-term trend in the tropospheric CRII over the last 6000 years. We note that wandering of the geomagnetic dipole axis, which is crucially important in centennial changes of CRII at middle latitudes (Kovaltsov and Usoskin, 2007; Usoskin et al., 2008), is not a dominant factor at the multi-millennial time scale. Instead, the slow changes of the geomagnetic dipole moment become very important in the tropics. The long-term trend in regional CRII can be quite strong—up to a factor of 1.5 variations at the equator (see Fig. 1E). Interestingly, the trends have different slopes in different regions, viz. the CRII was increasing in polar areas and decreasing in tropics. This fact makes it possible to perform a statistical test of a relation between CRII and local/regional climate reconstructions.

The global effect of CR upon Earth is defined, at the studied time scale of several millennia, largely by changes in the geomagnetic field rather than by solar variability, which can lead to an unsettled effect of the apparent solar variability on climate (e.g., Bard and Frank, 2006). On the other hand, this may help in disentangling direct solar effects (e.g., via the irradiance) from those caused by CR via the heliospheric modulation.

As an illustration of the possible climate implication we have compared the reconstructed changes of the status of lakes around the world with the CRII trend pattern for the last 6–7 millennia. The agreement between them is significant—the probability of a random coincidence is estimated as 2%. At first glance, even such a formally significant agreement may be casual not serving as an evidence for a real link, because different trends in regional climate between tropics and polar regions can be an intrinsic feature of the global climate system. If so, detailed models of the climate dynamics throughout the Holocene, using a general circulation model (GSM), would predict patterns comparable with the map of lake status changes (Schmidt et al., 2004). Note, however, that results of such direct models, that include only the direct solar forcing, did not yield general agreement with the observed lake status features (Kohfeld and Harrison, 2000; Sawada et al., 2004). Therefore, it appears plausible to think that the good agreement between CRII and lake status patterns implies a real connection, viz. that changes in CRII may slightly modulate the local climate. A similar conclusion has been drawn recently by Knudsen and Riisager (2009) for China and Oman regional speleothem precipitation data over the Holocene. However, this does not imply that the other, direct, mechanisms via, e.g., solar

insolation are less important. Further studies using other climate parameters are necessary to investigate particular mechanisms of the CRII climate relation, which is not attempted here.

Concluding, we have demonstrated that:

- Long-term (multi-millennial) trends of the cosmic ray induced ionization in the troposphere are defined not only by solar (i.e., covariant with solar irradiance) changes but largely by changes of the geomagnetic field.
- CRII variations are not spatially homogeneous but they depict a clear geographical pattern. This is particularly important in tropical regions and for global averaged data.
- Ionization in the polar region is mostly affected by the solar variability.

An analysis of spatio-temporal relation between the modeled ionization trends and the lake level data as an example of the regional climate change on the time scale of 6–7 millennia reveals a statistically significant correlation between them, which appears better than the results of direct general circulation modeling considering only the direct solar forcing.

This suggests that CRII may play a role in long-term regional climate variations. The next step would be to include a geographical time-dependent effect of CRII into general circulation models, in addition to all other known effects, such as orbital forcing or solar irradiance variations, in an attempt to model the corresponding observed patterns.

Acknowledgments

Supports from the Academy of Finland and the Finnish Academy of Science and Letters Vilho, Yrjö and Kalle Väisälä Foundation are acknowledged. GAK was partly supported by the Program of Presidium RAS N16-3-5.4. IM acknowledges two Grants (RNP.2.1.1.4166 and RNP.2.2.1.1.3836) of the Russian Ministry of Education and Science.

Appendix A. Computation of the geomagnetic cutoff rigidity

Although computation of the geomagnetic cutoff rigidity in the eccentric dipole approximation of the geomagnetic field is straightforward using vector algebra and spherical geometry, it is lengthy and laborious. Since we are not aware of a detailed published recipe for such a computation, we give its essentials here.

In order to totally describe the geomagnetic field in the eccentric dipole approximation (see full details in Fraser-Smith, 1987), one needs the first eight Gauss coefficients of the magnetic field decomposition (for the centered dipole, only three coefficients are sufficient). The eccentric dipole is assumed to possess the same magnetic dipole moment M and the same orientation of the magnetic axis as the centered dipole, but its center is displaced with respect to the Earth's center.

Let us consider a system of orthogonal Cartesian coordinates (x, y, z) with the origin at the Earth's center, so that the z -axis coincides with the Earth's rotational axis, the x -axis points to the crossing of the Greenwich meridian and the Equator, and the y -axis completes the right-hand system. In this reference frame let us define a system of spherical coordinates (r, θ, ψ) whose polar angle coincides with the z -axis.

The dipole moment is defined using the first three Gauss coefficients, g_0^1, g_1^1, h_1^1 , as

$$M = \frac{4\pi}{\mu_0} B_0 R_0^3 \quad (\text{A.1})$$

where μ_0 is the free space magnetic permeability and R_0 is the mean radius of Earth, and

$$B_0^2 = (g_1^0)^2 + (g_1^1)^2 + (h_1^1)^2. \quad (\text{A.2})$$

Let us denote vector

$$\mathbf{p} \left(-\frac{g_1^1}{B_0}, -\frac{h_1^1}{B_0}, -\frac{g_1^0}{B_0} \right)$$

as the direction of the dipole axis (the same for centered and eccentric dipole), and vector $\mathbf{d}(x_0; y_0; z_0)$ as the vector from the Earth's center to the center of eccentric dipole.

$$\frac{x_0}{R_0} = \frac{L_1 - g_1^1 E}{3B_0^2};$$

$$\frac{y_0}{R_0} = \frac{L_2 - h_1^1 E}{3B_0^2};$$

$$\frac{z_0}{R_0} = \frac{L_0 - g_1^0 E}{3B_0^2}, \quad (\text{A.3})$$

where

$$L_0 = 2g_1^0 g_2^0 + \sqrt{3}(g_1^1 g_2^1 + h_1^1 h_2^1),$$

$$L_1 = -g_1^0 g_2^0 + \sqrt{3}(g_1^0 g_2^1 + g_1^1 g_2^2 + h_1^1 h_2^2),$$

$$L_2 = -h_1^1 g_2^0 + \sqrt{3}(g_1^0 h_2^1 - h_1^1 g_2^2 + g_1^1 h_2^2),$$

$$E = \frac{L_0 g_1^0 + L_1 g_1^1 + L_2 h_1^1}{4B_0^2}.$$

Let us define $\mathbf{r}(R_0 \sin \theta \cos \psi; R_0 \sin \theta \sin \psi; R_0 \cos \theta)$ as a vector from the Earth's center to the observational point with geographical co-latitude θ and longitude ψ on the surface. Let $\mathbf{R} = \mathbf{r} - \mathbf{d}$ be the vector from the center of the eccentric dipole to this observational point. The squared distance between the eccentric dipole center and the observational point is

$$R^2 = R_0^2 + d^2 - 2R_0(x_0 \sin \theta \cos \psi + y_0 \sin \theta \sin \psi + z_0 \cos \theta). \quad (\text{A.4})$$

The geomagnetic co-latitude, i.e., the angle between the magnetic dipole axis and vector \mathbf{R} , $\theta_G = 90^\circ - \lambda_G$, can be defined as

$$\cos \theta_G = \frac{\mathbf{R} \cdot \mathbf{p}}{R p} = \frac{1}{R B_0} [g_1^1(x_0 - R_0 \sin \theta \cos \psi) + h_1^1(y_0 - R_0 \sin \theta \sin \psi) + g_1^0(z_0 - R_0 \cos \theta)]. \quad (\text{A.5})$$

Finally, the vertical geomagnetic cutoff rigidity can be calculated using Störmer's equation (Eq. (2)) as

$$Pc = 1.9 \cdot M \left(\frac{R_0}{R} \right)^2 \sin^4 \theta_G, \quad (\text{A.6})$$

where Pc and M are given in GV and in 10^{22} Am², respectively. Thus computed cutoff rigidity has been used in the computations presented in this paper.

References

- Arnold, F., 2008. Atmospheric ions and aerosol formation. *Space Sci. Rev.* 137, 225–239.
- Bard, E., Frank, M., 2006. Climate change and solar variability: what's new under the sun? *Earth Planet. Sci. Lett.* 248, 1–14.
- Bazilevskaya, G.A., Usoskin, I.G., Flückiger, E.O., Harrison, R.G., Desorgher, L., Büttikofer, R., Krainev, M.B., Makhmutov, V.S., Stozhkov, Y.I., Svirzhetskaya, A.K., Svirzhetsky, N.S., Kovaltsov, G.A., 2008. Cosmic ray induced ion production in the atmosphere. *Space Sci. Rev.* 137, 149–173.
- Bond, G., Kromer, B., Beer, J., Muscheler, R., Evans, M.N., Showers, W., Hoffmann, S., Lotti-Bond, R., Hajdas, I., Bonani, G., 2001. Persistent solar influence on North Atlantic climate during the Holocene. *Science* 294, 2130–2136.

- Christl, M., Mangini, A., Holzkaemper, S., Spötl, C., 2004. Evidence for a link between the flux of galactic cosmic rays and Earth's climate during the past 200,000 years. *J. Atmos. Sol. Terr. Phys.* 66, 313–322.
- Cooke, D., Humble, J., Shea, M., Smart, D., Lund, N., Rasmussen, I., Byrnek, B., Gore, P., Petrou, N., 1991. On cosmic-ray cut-off terminology. *Nuovo Cim. C* 14, 213–234.
- Courtilot, V., Gallet, Y., Le Mouél, J.-L., Fluteau, F., Genevey, A., 2007. Are there connections between the Earth's magnetic field and climate? *Earth Planet. Sci. Lett.* 253, 328–339.
- de Jager, C., 2005. Solar forcing of climate. 1: solar variability. *Space Sci. Rev.* 120, 197–241.
- Dorman, L., 2004. *Cosmic Rays in the Earth's Atmosphere and Underground*. Kluwer Academic Publishers, Dordrecht, Netherlands.
- Elsasser, W., Nay, E., Winkler, J., 1956. Cosmic-ray intensity and geomagnetism. *Nature* 178, 1226–1227.
- Foukal, P., Fröhlich, C., Spruit, H., Wigley, T., 2006. Variations in solar luminosity and their effect on the earth's climate. *Nature* 443, 161–166.
- Fraser-Smith, A.C., 1987. Centered and eccentric geomagnetic dipoles and their poles 1600–1985. *Rev. Geophys.* 25, 1–16.
- Gallet, Y., Genevey, A., Fluteau, F., 2005. Does Earth's magnetic field secular variation control centennial climate change? *Earth Planet. Sci. Lett.* 236, 339–347.
- Gallet, Y., Genevey, A., Le Goff, M., Fluteau, F., Ali Eshraghi, S., 2006. Possible impact of the Earth's magnetic field on the history of ancient civilizations. *Earth Planet. Sci. Lett.* 246, 17–26.
- Haigh, J.D., Blackburn, M., 2006. Solar influences on dynamical coupling between the stratosphere and troposphere. *Space Sci. Rev.* 125, 331–344.
- Haigh, J.D., Lockwood, M., Giampapa, M.S., 2005. The Sun. In: Rüedi, I., Güdel, M., Schmutz, W. (Eds.), *Saas-Fee Advanced Course 34: The Sun Solar Analogs and the Climate*. Springer, Berlin.
- Harrison, S.P., Kutzbach, J.E., Liu, Z., Bartlein, P.J., Otto-Bliesner, B., Muhs, D., Prentice, I.C., Thompson, R.S., 2003. Mid-Holocene climates of the America: a dynamical response to changed seasonality. *Clim. Dyn.* 20, 663–688.
- Hong, Y.T., Wang, Z.G., Jiang, H.B., Lin, Q.H., Hong, B., Zhu, Y.X., Wang, Y., Xu, L.S., Leng, X.T., Li, H.D., 2001. A 6000-year record of changes in drought and precipitation in northeastern China based on a $\delta^{13}\text{C}$ time series from peat cellulose. *Earth Planet. Sci. Lett.* 185, 111–119.
- Hyodo, M., Biswas, D.K., Noda, T., Tomioka, N., Mishima, T., Itota, C., Sato, H., 2006. Millennial- to submillennial-scale features of the Matuyama–Brunhes geomagnetic polarity transition from Osaka Bay, southwestern Japan. *J. Geophys. Res.* 111, B02103.
- Kazil, J., Harrison, R.G., Lovejoy, E.R., 2008. Tropospheric new particle formation and the role of ions. *Space Sci. Rev.* 137, 241–255.
- Kazil, J., Lovejoy, E.R., Barth, M.C., O'Brien, K., 2006. Aerosol nucleation over oceans and the role of galactic cosmic rays. *Atmos. Chem. Phys.* 6, 4905–4924.
- Kitaba, I., Iwabe, C., Hyodo, M., Katoh, S., Matsushita, M., 2009. High-resolution climate stratigraphy across the Matuyama–Brunhes transition from palynological data of Osaka Bay sediments in southwestern Japan. *Palaeogeograph. Palaeoclim. Palaeoecol.* 272, 115–123.
- Knudsen, M., Riisager, P., 2009. Is there a link between earth's magnetic field and low-latitude precipitation? *Geology* 37, 71–74.
- Kohfeld, K., Harrison, S., 2000. How well can we simulate past climates? Evaluating the models using global palaeoenvironmental datasets. *Quatern. Sci. Rev.* 19, 321–346.
- Korte, M., Constable, C., 2005. Continuous geomagnetic field models for the past 7 millennia: 2. CALS7K. *Geochem. Geophys.* 6, Q02H16.
- Korte, M., Constable, C., 2008. Spatial and temporal resolution of millennial scale geomagnetic field models. *Adv. Space Res.* 41, 57–69.
- Kovaltsov, G.A., Usoskin, I.G., 2007. Regional cosmic ray induced ionization and geomagnetic field changes. *Adv. Geosci.* 13, 31–35.
- Kudela, K., Usoskin, I.G., 2004. On Magnetospheric Transmissivity of Cosmic Rays. *Czech. J. Phys.* 54, 239–254.
- Marsh, N., Svensmark, H., 2003. Solar influence on Earth's climate. *Space Sci. Rev.* 107, 317–325.
- Mironova, I.A., Desorgher, L., Usoskin, I.G., Flückiger, E.O., Bütikofer, R., 2008. Variations of aerosol optical properties during the extreme solar event in January 2005. *Geophys. Res. Lett.* 35, L18610.
- Niggemann, S., Mangini, A., Mudelsee, M., Richter, D.K., Wurth, G., 2003. Sub-Milankovitch climatic cycles in Holocene stalagmites from Sauerland, Germany. *Earth Planet. Sci. Lett.* 216, 539–547.
- Pallé, E., Butler, C.J., O'Brien, K., 2004. The possible connection between ionization in the atmosphere by cosmic rays and low level clouds. *J. Atmos. Sol. Terr. Phys.* 66, 1779–1790.
- Sawada, M., Viau, A.E., Vettoretti, G., Peltier, W.R., Gajewski, K., 2004. Comparison of North-American pollen-based temperature and global lake-status with CCCma AGCM2 output at 6 ka. *Quatern. Sci. Rev.* 23, 225–244.
- Scherer, K., Fichtner, H., Borrmann, T., Beer, J., Desorgher, L., Flückiger, E., Fahr, H.-J., Ferreira, S.E.S., Langner, U.W., Potgieter, M.S., Heber, B., Masarik, J., Shaviv, N., Veizer, J., 2006. Interstellar–terrestrial relations: variable cosmic environments, the dynamic heliosphere, and their imprints on terrestrial archives and climate. *Space Sci. Rev.* 127, 327–465.
- Schmidt, G.A., Shindell, D.T., Miller, R.L., Mann, M.E., Rind, D., 2004. General circulation modelling of Holocene climate variability. *Quatern. Sci. Rev.* 23, 2167–2181.
- Smart, D.F., Shea, M.A., Flückiger, E.O., 2000. Magnetospheric models and trajectory computations. *Space Sci. Rev.* 93, 305–333.
- Tinsley, B.A., 2008. The global atmospheric electric circuit and its effects on cloud microphysics. *Rep. Prog. Phys.* 71, 066801.
- Usoskin, I., Schüssler, M., Solanki, S., Mursula, K., 2005a. Solar activity, cosmic rays, and earth's temperature: a millennium-scale comparison. *J. Geophys. Res.* 110, A10102.
- Usoskin, I.G., Alanko-Huotari, K., Kovaltsov, G.A., Mursula, K., 2005b. Heliospheric modulation of cosmic rays: monthly reconstruction for 1951–2004. *J. Geophys. Res.* 110, A12108.
- Usoskin, I.G., Desorgher, L., Velinov, P., Storini, M., Flückiger, E.O., Bütikofer, R., Kovaltsov, G.A., 2009. Ionization of the earth's atmosphere by solar and galactic cosmic rays. *Acta Geophys.* 57, 88–101.
- Usoskin, I.G., Gladysheva, O.G., Kovaltsov, G.A., 2004. Cosmic ray-induced ionization in the atmosphere: spatial and temporal changes. *J. Atmos. Sol. Terr. Phys.* 66, 1791–1796.
- Usoskin, I.G., Korte, M., Kovaltsov, G.A., 2008. Role of centennial geomagnetic changes in local atmospheric ionization. *Geophys. Res. Lett.* 35, L05811.
- Usoskin, I.G., Kovaltsov, G.A., 2004. Long-term solar activity: direct and indirect study. *Solar Phys.* 224, 37–47.
- Usoskin, I.G., Kovaltsov, G.A., 2006. Cosmic ray induced ionization in the atmosphere: full modeling and practical applications. *J. Geophys. Res.* 111, D21206.
- Usoskin, I.G., Kovaltsov, G.A., 2008. Cosmic rays and climate of the Earth: possible connection. *C. R. Geosci.* 340, 441–450.
- Usoskin, I.G., Solanki, S.K., Kovaltsov, G.A., 2007. Grand minima and maxima of solar activity: new observational constraints. *Astron. Astrophys.* 471, 301–309.
- Usoskin, I.G., Voiculescu, M., Kovaltsov, G.A., Mursula, K., 2006. Correlation between clouds at different altitudes and solar activity: fact or artifact? *J. Atmos. Sol. Terr. Phys.* 68, 2164–2172.
- Van Geel, B., Raspopov, O., Renssen, H., Van der Plicht, J., Dergachev, V., Meijer, H., 1999. The role of solar forcing upon climate change. *Quatern. Sci. Rev.* 18, 331–338.
- Versteegh, G., 2005. Solar forcing of climate. 2: evidence from the past. *Space Sci. Rev.* 120, 243–286.
- Voiculescu, M., Usoskin, I.G., Mursula, K., 2006. Different response of clouds to solar input. *Geophys. Res. Lett.* 33, L21802.
- Webber, W., 1962. Time variations of low rigidity cosmic rays during the recent sunspot cycle. In: Wilson, J., Wouthuysen, S. (Eds.), *Progress in Elementary Particle and Cosmic Ray Physics*, vol. 6. North-Holland, Amsterdam, pp. 77–243.
- Xiao, J., Nakamura, T., Lu, H., Zhang, G., 2002. Holocene climate changes over the desert/loess transition of north-central China. *Earth Planet. Sci. Lett.* 197, 11–18.
- Yu, G., Harrison, S., Xue, B., 2001. Lake status records from china: data base documentation. Technical Reports 4, Max-Planck-Institut für Biogeochemie, Germany.